Rab7b controls trafficking from endosomes to the TGN

Cinzia Progida[1,2], Laura Cogli[1], Francesco Piro[1], Azzurra De Luca[1], Oddmund Bakke[2,3] and Cecilia Bucci[1,*]

[1]Department of Biological and Environmental Sciences and Technologies (DiSTeBA), University of Salento, Via Provinciale Monteroni, 73100 Lecce, Italy
[2]Centre for Immune Regulation, Department of Molecular Biosciences, University of Oslo, 0316 Oslo, Norway
[3]The Gade Institute, University of Bergen, 5021 Bergen, Norway
*Author for correspondence (cecilia.bucci@unisalento.it)

Accepted 10 February 2010
Journal of Cell Science 123, 1480-1491

doi:10.1242/jcs.051474

Summary

Rab7b is a recently identified member of the Rab GTPase protein family and has high similarity to Rab7. It has been reported that Rab7b is lysosome associated, that it is involved in monocytic differentiation and that it promotes lysosomal degradation of TLR4 and TLR9. Here we investigated further the localization and function of this GTPase. We found that wild-type Rab7b is lysosome associated whereas an activated, GTP-bound form of Rab7b localizes to the Golgi apparatus. In contrast to Rab7, Rab7b is not involved in EGF and EGFR degradation. Depletion of Rab7b or expression of Rab7b T22N, a Rab7b dominant-negative mutant, impairs cathepsin-D maturation and causes increased secretion of hexosaminidase. Moreover, expression of Rab7b T22N or depletion of Rab7b alters TGN46 distribution, cation-independent mannose-6-phosphate receptor (CI-MPR) trafficking, and causes an increase in the levels of the late endosomal markers CI-MPR and cathepsin D. Vesicular stomatitis virus G protein (VSV-G) trafficking, by contrast, is normal in Rab7b-depleted or Rab7b-T22N-expressing cells. In addition, depletion of Rab7b prevents cholera toxin B-subunit from reaching the Golgi. Altogether, these data indicate that Rab7b is required for normal lysosome function, and, in particular, that it is an essential factor for retrograde transport from endosomes to the trans-Golgi network (TGN).

Key words: Rab proteins, Rab7, Rab7b, Endosomes, Lysosomes, Lysosomal enzymes

Introduction

Rab proteins are important regulators of all aspects of membrane trafficking (Cai et al., 2007; Grosshans et al., 2006; Markgraf et al., 2007). Indeed, they are monomeric GTPases that regulate vesicle formation, vesicle transport on microtubules, tethering, docking, and fusion of membranes (Pfeffer, 2005a; Pfeffer, 2005b; Seabra and Wasmeier, 2004). Rab proteins control transport steps by cycling between an active GTP-bound and an inactive GDP-bound form. To function, active Rab proteins must associate with cellular membranes. Indeed, Rabs are post-translationally modified by geranyl-geranylation, which is responsible for their membrane anchorage (Pereira-Leal et al., 2001).

In mammalian cells, there are more than 60 different Rab proteins, consistent with the high complexity of intracellular vesicular trafficking in these organisms. Each Rab protein has a specific intracellular location and is involved in the regulation of a different step of vesicular transport. Some Rab proteins exist in multiple isoforms, share high sequence identity and seem to have the same cellular functions. Five mammalian Rab-specific regions, useful in defining a Rab protein by using its primary structure, have been identified and called Rab-family motifs (RabF) (Pereira-Leal and Seabra, 2000). In addition, four other regions, identified as Rab-subfamily-specific sequences and called Rab-subfamily regions (RabSF), define Rab subfamilies (Moore et al., 1995; Pereira-Leal and Seabra, 2000; Pereira-Leal and Seabra, 2001). On the basis of these primary-structure studies on Rab proteins, it was proposed that, in order to classify Rab proteins as isoforms, their sequences should be at least 70% identical, there should be conservation of the RabF and RabSF motifs, and the proteins should also show specific characteristics (Pereira-Leal and Seabra, 2000; Pereira-Leal and Seabra, 2001).

Rab7 is a small GTPase that controls transport towards late endosomes and lysosomes (Bucci et al., 2000; Press et al., 1998; Vitelli et al., 1997). Rab7 regulates epithelial growth factor (EGF) and EGF receptor (EGFR) degradation, trafficking of the nerve-growth-factor receptor TrkA, phagosome maturation and autophagy (Ceresa, 2006; Deinhardt et al., 2006; Gutierrez et al., 2004; Harrison et al., 2003; Jager et al., 2004; Saxena et al., 2005). In addition, Rab7 has recently been shown to participate in the regulation of the retromer recruitment onto endosomes (Rojas et al., 2008). Rab7 catalyzes these processes by binding to specific effectors, including Rabring 7, the small GTPase Rac1, the phosphatidylinositol 30-kinase VPS34 and its adaptor protein p150, the proteasome α-subunit XAPC7, the oxysterol-binding protein homologue ORP1L, PRA1, the *Entamoeba histolytica* VPS26, and the Rab-interacting lysosomal protein RILP (Bucci et al., 1999; Cantalupo et al., 2001; Dong et al., 2004; Johansson et al., 2005; Mizuno et al., 2003; Nakada-Tsukui et al., 2005; Sakane et al., 2007; Stein et al., 2003; Sun et al., 2005).

Recently, a Rab protein that shares about 50% identity and 65% similarity with Rab7 has been identified and named Rab7b (Yang et al., 2004). Rab7b is mainly expressed in monocytes, monocyte-derived dendritic cells and promyeloid or monocytic leukaemia cell lines, and it colocalizes with LAMP1-positive compartments and with Toll-like receptor 4 (TLR4) upon lipopolysaccharide (LPS) treatment (Wang et al., 2007; Yang et al., 2004). In addition, Rab7b regulates TLR4 and TLR9 trafficking and degradation, thereby modulating TLR4 and TLR9 signalling (Wang et al., 2007; Yang et al., 2004; Yao et al., 2009). Here, we further investigated Rab7b expression, localization and function in comparison with Rab7. We made use of dominant-negative Rab7b T22N and constitutively active Rab7b Q67L mutants, and we depleted cells of Rab7b using RNA interference to investigate Rab7b function.

Our data indicate that Rab7b functions in the transport steps between endosomes and the trans-Golgi network (TGN).

Results

Rab7b is expressed in HeLa cells

Rab7b cDNA has been previously isolated from dendritic cells and the *Rab7b* gene was reported to be specifically expressed in promyeloid or monocytic leukaemia cell lines (Yang et al., 2004). To confirm this, we extracted RNA from HeLa, U-937 and THP-1 human cell lines. After retro-transcription, we performed quantitative real-time PCR using *Rab7b*-specific primers and β-actin primers as control. We found that *Rab7b* mRNA was also expressed in HeLa cells, although at a lower level than in U937 and THP-1 cells (Fig. 1A,B). Rab7b expression in HeLa cells was also silenced using specific siRNAs. Quantitative real-time PCR showed that *Rab7b* mRNA expression is reduced to about 20% compared with control cells (Fig. 1A,B). By contrast, no reduction was observed if control RNA oligonucleotides were used (data not shown). The level of Rab7b was also measured by western blotting. Analysis of different cell lysates revealed that the expression level of Rab7b was too low to be detected in HeLa cells with the available antibodies. By contrast, we could detect expression of Rab7b in U937, THP-1 and dendritic cells, confirming real-time PCR data carried out on mRNA (Fig. 1C). To compare Rab7 and Rab7b expression, we incubated the same membrane with an antibody directed against Rab7, revealing that Rab7 is also more highly expressed in THP-1 and dendritic cells compared with HeLa cells (Fig. 1C). Silencing was effective also in U-937 and THP-1 cells as shown in Fig. 1D. In addition, we verified that the silencing of Rab7b did not affect the expression of other similar Rab proteins. Western blot analysis on *Rab7b*-silenced HeLa and U937 cells demonstrated that Rab7 or Rab9 levels did not change, indicating that the silencing is specific and that the expression level of these Rab proteins were not directly affected by silencing Rab7b (Fig. 1E and data not shown).

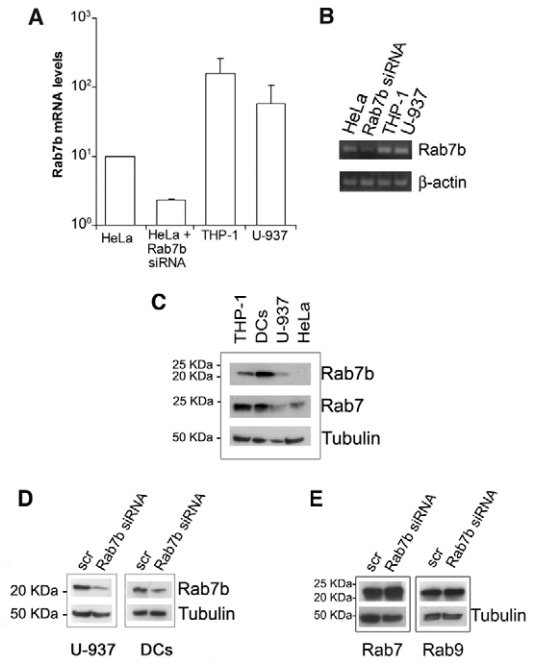

Fig. 1. Rab7b expression in human cell lines. (**A**) *Rab7b* mRNA levels were quantified in different human cell lines (HeLa, THP-1 and U937) and in Rab7b-depleted HeLa cells by real-time reverse-transcriptase (RT)-PCR. (**B**) PCR products amplified by real-time RT-PCR were analyzed by agarose gel electrophoresis. β-actin primers were used as control. Each real-time RT-PCR experiment was repeated three times using distinct cDNA preparations for each RNA sample. (**C**) Rab7b and Rab7 protein levels were analyzed in different human cell lines [THP-1, monocyte-derived dendritic cells (DCs), U937 and HeLa] by western blotting. (**D**) U937 and DCs were treated with control RNA (scr) or siRNA against *Rab7b*. Cell lysates were analyzed by western blotting with antibodies against Rab7b or tubulin (as loading control). (**E**) U937 cells transfected with control RNA (scr) or siRNA against *Rab7b*, were lysed and analyzed by western blotting with antibodies against Rab7 or Rab9. Antibody against tubulin was used to verify equal loading.

Rab7b is localized to the TGN and late endosomes

In order to establish the intracellular localization of Rab7b, we used specific monoclonal and polyclonal commercial antibodies for immunofluorescence analysis. We were not able to detect the Rab7b protein by immunofluorescence in HeLa cells, probably owing to its low expression. The staining on THP-1 and U-937 cells confirmed that the endogenous Rab7b protein colocalized partially with late endosomal and/or lysosomal markers such as Lamp1 and with CI-MPR. Surprisingly, Rab7b also colocalized, although to lesser extent, with TGN46 (Fig. 2; supplementary material Fig. S1, and data not shown).

Then we examined the intracellular localization of overexpressed GFP- or HA-tagged Rab7b using different antibodies for the staining of intracellular compartments in U937, Raw 264.7 and HeLa cells (Figs 2, 3; supplementary material Figs S2-S4, and data not shown). No colocalization of the overexpressed protein was ever seen with early endosomal markers such as EEA1 or transferrin receptor, whereas a partial colocalization was observed with the late endosomal and/or lysosomal markers Lamp1, Lamp2 and CD63 (Figs 2, 3; supplementary material Fig. S4, and data not shown), as previously shown (Wang et al., 2007). Interestingly, we found, in addition, a partial colocalization with TGN and Golgi markers, such as giantin (GCP372), Golgin-97, TGN46 and Golgin-245 (Figs 2, 3; supplementary material Figs S2-S4, and data not shown). The colocalization with Golgi and TGN markers was more conspicuous with the constitutively active mutant GFP–Rab7b-Q67L (Figs 2, 3; supplementary material Figs S2-S4). Indeed, this mutant showed a high degree of colocalization with TGN46, Golgin-245 and giantin not only when expressed in HeLa cells (Fig. 3; supplementary material Fig. S3) but also in U-937 and RAW264.7 cells (Fig. 2; supplementary material Figs S2, S4). No colocalization of Rab7 or of Rab7-Q67L with the same markers was ever observed (supplementary material Fig. S5, and data not shown). To further confirm the localization of the Rab7b-Q67L mutant protein, HeLa cells were treated with brefeldin A (BFA) to disrupt the Golgi complex (Ward et al., 2001). After treatment, cells were stained with anti-giantin antibody (Fig. 3). In cells treated with BFA, in which the Golgi complex was disrupted as expected, Rab7b-Q67L localization was dramatically altered compared with control cells, even at early time points (Fig. 3).

Next, we examined the effects of expression of the Rab7b-T22N dominant-negative mutant on the intracellular distribution of various markers in HeLa cells (Fig. 4A). Although no effects were detected on early or late endosomal markers, the distribution of TGN46 was dramatically altered. Indeed, in cells expressing the Rab7b-T22N mutant, TGN46 did not show its characteristic staining concentrated on one side of the nucleus but showed a vesicular staining dispersed

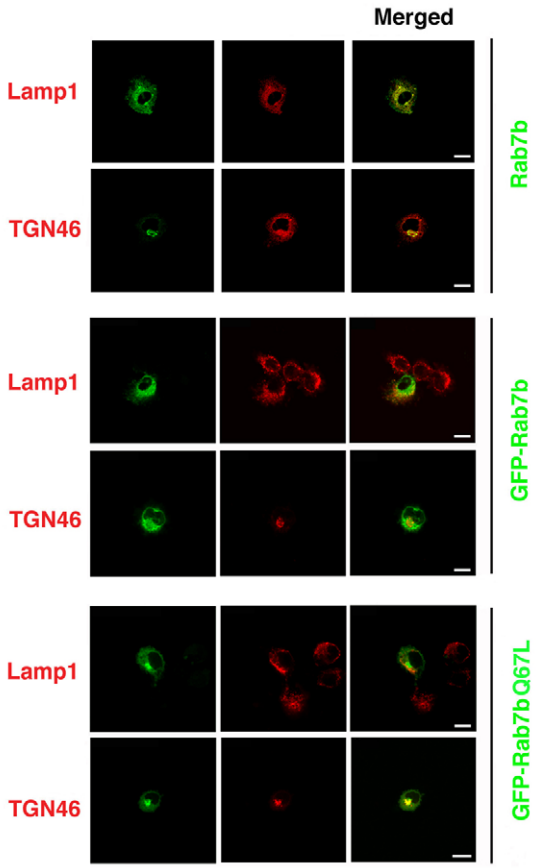

Fig. 2. Immunofluorescence analysis of Rab7b localization in U937 cells. (Top) U937 human monocytic cells differentiated in macrophages with phorbol myristate acetate (PMA) were fixed, permeabilized and stained with antibodies against Rab7b and Lamp1 or TGN46 in combination with a Cy3- and FITC-conjugated secondary antibody. (Middle and lower) U937 cells transfected with wild-type *GFP-Rab7b* or *GFP–Rab7b-Q67L* as indicated, after fixation and permeabilization, were stained with antibodies against Lamp1 or TGN46 in combination with a Cy3-conjugated secondary antibody. Merged images of the different channels are shown in the last column. Scale bars: 10 µm.

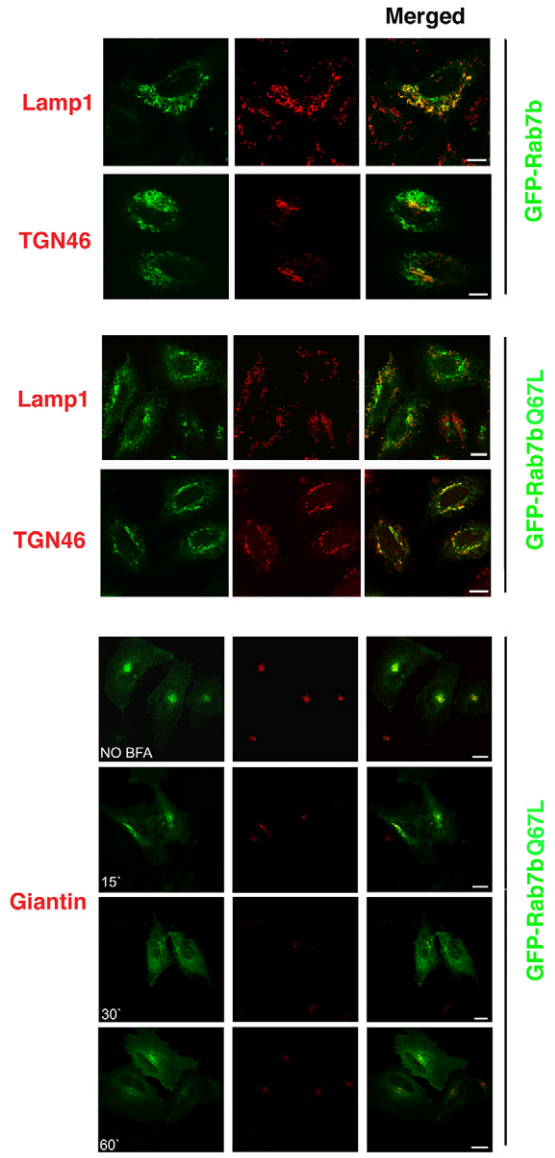

Fig. 3. Immunofluorescence analysis of Rab7b localization in HeLa cells. HeLa cells were transfected with wild-type *GFP-Rab7b* or *GFP–Rab7b-Q67L* and, after fixation and permeabilization, were stained with antibodies against Lamp1 or TGN46 in combination with a Cy3-conjugated secondary antibody. As indicated in the bottom set of images, HeLa cells transfected with *GFP–Rab7b-Q67L* were incubated for different time points with BFA (1 µg/ml) before immunofluorescence analysis. After fixation and permeabilization, cells were stained with anti-giantin antibody in combination with a Cy3-conjugated secondary antibody. In the presence of BFA, Rab7b-Q67L and giantin distribution is altered. Merged images of the different channels are shown in the last column. Scale bars: 10 µm.

in the entire cell (Fig. 4A). Similarly, giantin also changed its distribution but only in cells expressing a high amount of the Rab7b-T22N protein (Fig. 4A; data not shown).

To test this finding by an alternative approach, we used Rab7b-silenced cells. Depletion of Rab7b in HeLa or U937 cells caused dispersion of TGN46, whereas no changes in giantin and Golgin-245 distribution were detected (Fig. 4B,C). We verified, by western blotting, whether there was an alteration of TGN46 level in Rab7b-depleted cells (Fig. 4D). We detected a similar amount of the protein in both HeLa and U937 cells treated with siRNA against *Rab7b* compared to control cells, suggesting that Rab7b depletion only affects the distribution of TGN46 and not its expression.

Altogether, these data show that Rab7b is localized not only to the late endosomal and/or lysosomal compartment but also to the Golgi and TGN, and that it is important for the correct intracellular distribution of some TGN and Golgi markers. This was true for all cell lines tested, independently of the Rab7b level of endogenous expression.

Rab7b is not involved in EGF or EGFR degradation

Rab7 is involved in the regulation of the EGF- and EGFR-degradation pathway (Ceresa and Bahr, 2006; Vitelli et al., 1997). Therefore, we examined EGF degradation in cells transfected with Rab7b wild-type or mutant proteins to test whether Rab7 and Rab7b have similar functions. Control or transfected cells were incubated with 0.8 mg/ml rhodamine-labelled EGF for 1 hour at 4°C, washed and then reincubated for different

time points (from 15 minutes up to 3 hours) at 37°C. Immunofluorescence analysis was performed and EGF staining quantified (supplementary material Fig. S6A). After 3 hours, EGF was almost completely degraded in control cells as well as in cells transfected with the different Rab7b constructs. EGF was degraded with the same kinetics also in Rab7b-depleted cells (supplementary material Fig. S6A).

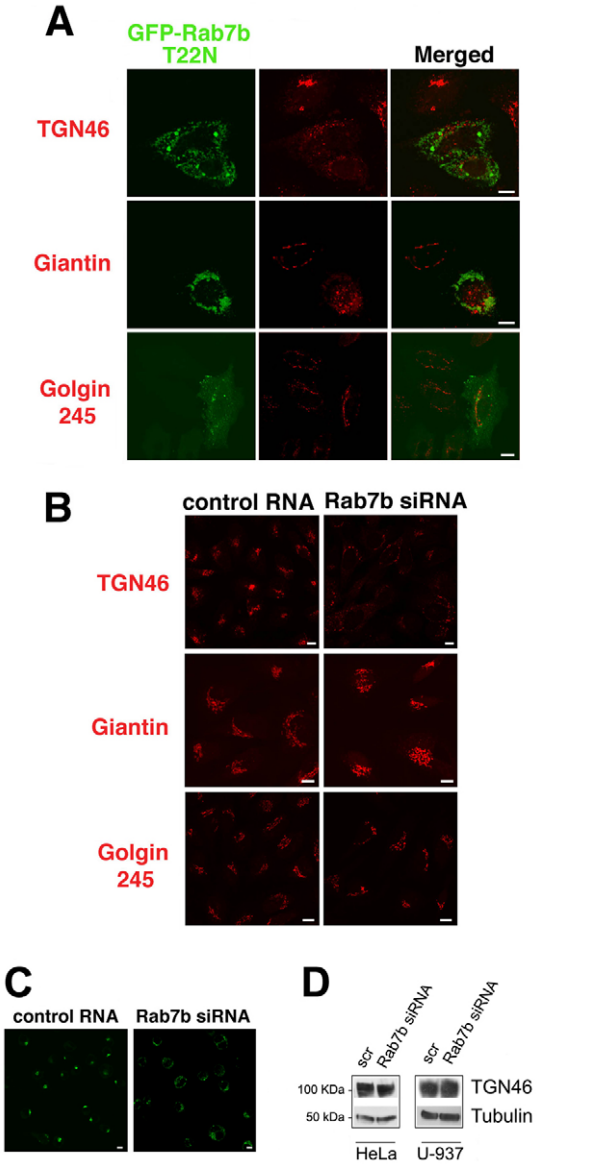

Fig. 4. Immunofluorescence analysis of cells expressing Rab7b T22N or of Rab7b-depleted cells. (**A**) HeLa cells were transfected with *Rab7b T22N* and subjected to immunofluorescence analysis using antibodies against TGN46, giantin or Golgin-245. The disruption of TGN46 and giantin staining is visible in cells expressing Rab7b T22N. (**B**) HeLa cells were treated with control RNA or *Rab7b* siRNA, as indicated in the Materials and Methods, and subjected to immunofluorescence analysis using antibodies against TGN46, giantin or Golgin-245. In Rab7b-silenced cells, TGN staining is dramatically altered. (**C**) U937 cells were transfected with control RNA or *Rab7b* siRNA and subjected to immunofluorescence analysis using anti-TGN46 antibody. (**D**) HeLa cells or U937 cells were treated with control RNA or *Rab7b* siRNA. Cell lysates were analyzed by western blotting against TGN46 or tubulin (as loading control). Scale bars: 10 μm.

This result was confirmed by measuring EGFR degradation by western blot analysis (supplementary material Fig. S6B-D). Control and transfected cells were incubated for 1 hour with 10 μg/ml cycloheximide to prevent new EGFR synthesis, and then with 50 ng/ml EGF for up to 3 hours. Cells were then lysed, and samples were resolved by SDS-PAGE and transferred onto membranes. Membranes were then incubated with anti-EGFR antibody; anti-tubulin antibody was used to verify equal loading of samples (supplementary material Fig. S6B,D). As shown in supplementary material Fig. S6, EGFR degradation was not influenced by the presence of any of the different Rab7b constructs.

Similar experiments were performed using Rab7b-depleted cells. Cells were transfected with control RNA, siRNA against *Rab7* or siRNA against *Rab7b*. As expected, almost complete EGFR degradation was observed in control cells, whereas a strong inhibition was detected in Rab7-depleted cells (supplementary material Fig. S6D). By contrast, Rab7b-depleted cells did not show any alteration of EGF degradation compared to control cells (supplementary material Fig. S6D).

In conclusion, unlike Rab7, Rab7b is not involved in the degradation of EGF nor EGFR, showing that the two Rab proteins have different roles.

Depletion of Rab7b increases hexosaminidase secretion

The intracellular localization of Rab7b prompted us to hypothesize that Rab7b could be involved in the trafficking of lysosomal enzymes. To test this hypothesis, we followed the trafficking of hexosaminidase (Riederer et al., 1994). This lysosomal enzyme is transported from the TGN to endosomes by mannose-6-phosphate receptors (MPRs). If CI-MPR transport is in some way blocked, an increased level of secretion via the bulk-flow default pathway of this enzyme should be observed. We treated HeLa cells with control RNA or siRNA against *Rab7b*, or we transfected them with the dominant-negative *Rab7b-T22N* mutant and measured the amount of newly synthesized hexosaminidase secreted in the presence of mannose 6-phosphate (M6P) to block interaction with receptors present on the cell surface (Fig. 5A). Interestingly, in Rab7b-depleted cells or in cells expressing Rab7b T22N, secretion of hexosaminidase was increased approximately twofold (Fig. 5A). In order to confirm that this effect was specifically due to Rab7b loss, we repeated the experiment in cells treated with siRNA

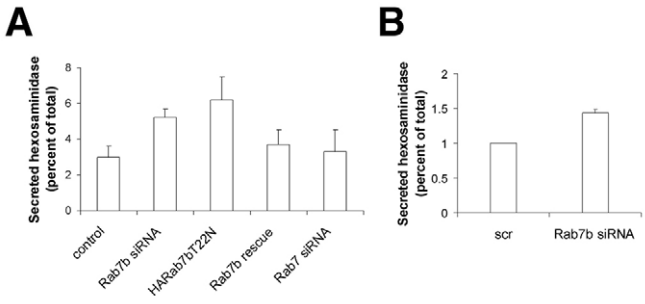

Fig. 5. Altered Rab7b function affects hexosaminidase sorting. (**A**) Control HeLa cells, HeLa cells transfected with siRNAs against *Rab7b*, *Rab7* or *GFP–Rab7b-T22N*, and HeLa cells depleted for Rab7b and transfected with HA-tagged *Rab7b* (Rab7b rescue) were incubated for 8 hours with 10 mM M6P. Secretion of hexosaminidase into medium was then measured. (**B**) Secretion of hexosaminidase was measured in U937 cells transfected with control siRNA or with siRNA against *Rab7b*. Results are expressed as percentage of the total cellular content of β-hexosaminidase.

against *Rab7* and in cells silenced for Rab7b, and then transfected them with HA-tagged *Rab7b*. In both cases, hexosaminidase secretion did not show any statistically significant alteration compared to control cells (Fig. 5A). Because HeLa cells express low levels of Rab7b, we measured hexosaminidase secretion also in cells that produce a higher amount of this protein. Similarly to HeLa cells, depletion of Rab7b in U937 cells also induced an increase in the secretion of hexosaminidase, although to a lesser extent (Fig. 5B), probably owing to a higher level of Rab7b after silencing in these cells compared with HeLa cells. The increased secretion of hexosaminidase in both HeLa and U937 cells depleted of Rab7b indicates that transport of lysosomal enzymes to endosomes is impaired, suggesting that Rab7b plays a role in the trafficking of lysosomal enzymes.

Depletion of Rab7b inhibits cathepsin-D maturation

To confirm these findings, we analyzed cathepsin-D maturation in Rab7b-depleted cells. Mature cathepsin D forms after proteolytic cleavages that occur in different intracellular compartments. Cathepsin D is synthesized as preprocathepsin-D precursor, which is converted into procathepsin D after the removal of the signal peptide in the endoplasmic reticulum (ER). Procathepsin D (52 kDa) is then transported to late endosomes and lysosomes and, encountering the acidic milieu, it undergoes further proteolytic processing. Indeed, it is slowly converted in to a 44-kDa form and finally into the 32-kDa mature form.

To follow cathepsin-D maturation, cells treated with control RNA or *Rab7b* siRNA were lysed, and proteins were subjected to SDS-PAGE, transferred to membranes and incubated with an anti-cathepsin-D antibody to detect the three forms of cathepsin D. In control cells, the procathepsin-D 52-kDa band was barely visible on blot and represented less than 5% of the total cathepsin-D staining, whereas the procathepsin-D 44-kDa band represented about 30% of the total amount (Fig. 6A,B). Upon depletion of Rab7b, the total amount of cathepsin D was increased, and the relative amount of the immature and mature forms changed. Indeed, the 52-kDa form was about fourfold more abundant (Fig. 6A,B). We verified that the difference in cathepsin-D levels was not due to off-target effects by transfecting Rab7b-silenced cells with *HA-Rab7b*. In these cells, the amount of cathepsin D and the relative amount of its different forms was very similar to control cells (Fig. 6A,B).

These data indicate that depletion of Rab7b impairs cathepsin-D maturation, suggesting that transport of cathepsin D from the TGN to endosomes, and subsequently to lysosomes, is impaired. In addition, the increased amount of cathepsin D in Rab7b-depleted cells suggests either a reduction in its degradation or an increase in cathepsin-D synthesis, which is often seen when lysosomal targeting is disrupted (Riederer et al., 1994).

Rab7b is not involved in VSV-G trafficking

To verify that Rab7b did not cause a general alteration in the secretory pathway, we followed VSV-G secretion in cells transfected with the Rab7b-T22N mutant or in cells depleted of Rab7b. After *YFP–VSV-G* transfection of cells pre-treated with control RNA, *Rab7b* siRNA or the *Rab7b-T22N* construct, cells were incubated at 39°C for 16 hours to allow VSV-G accumulation in the ER. Then cells were incubated at 32°C for 20 min or 1 h and the YFP–VSV-G present in the ER, Golgi or plasma membrane was scored by light microscopy (supplementary material Fig. S7). In control cells, after 20 minutes of incubation at 32°C, the majority of YFP–VSV-G was localized to the Golgi, whereas, at 60 minutes, YFP–VSV-G could be detected at the plasma membrane (supplementary material Fig. S7). Similar kinetics were observed in Rab7b-depleted cells and in cells transfected with plasmids encoding the Rab7b-T22N dominant-negative mutant protein (supplementary material Fig. S7, and data not shown).

These data strongly suggest that Rab7b is not involved in the trafficking between the ER and the plasma membrane.

Rab7b plays a role in CI-MPR transport

Western blot analysis of cathepsin D revealed that the amount of this lysosomal enzyme was increased in Rab7b-depleted cells (Fig. 6A,B).

Immunofluorescence analysis of Rab7b-depleted cells with anti-CI-MPR antibodies showed a marked increase in the staining of this receptor also (Fig. 7A). Quantitative confocal microscopy of the signal on multiple cells confirmed this finding (Fig. 7B). Indeed, CI-MPR showed an increase of about 40% in its total intensity when Rab7b was depleted (Fig. 7B). Under the same conditions, no changes were detected for giantin and Golgin-245 signals (see Fig. 4B; data not shown). CI-MPR staining in Rab7b-depleted cells also showed a more dispersed localization compared with control cells (Fig. 7A). The results obtained for the CI-MPR were confirmed by western blot analysis as shown in Fig. 7C.

Quantification indicated that absolute cellular levels of CI-MPR increased more than twofold in cells depleted of Rab7b, consistent with the data obtained by confocal quantitative immunofluorescence (Fig. 7D). These results suggest that cells compensate for a block in CI-MPR transport by upregulating lysosomal enzymes.

We then analyzed synthesis and turnover of CI-MPR in control cells and Rab7b-depleted cells. Cells were metabolically labelled

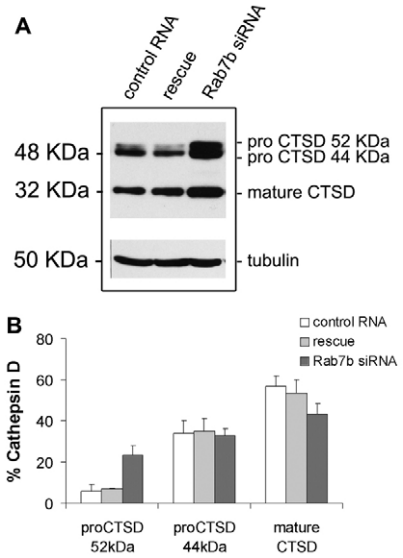

Fig. 6. Rab7b depletion inhibits cathepsin-D maturation. (**A**) Western blot analysis of cathepsin D was determined in HeLa cells transfected with either control RNA or siRNA against *Rab7b*, or depleted for Rab7b, and then transfected with HA-tagged *Rab7b* (rescue). Precursor (pro CTSD 52 kDa), intermediate (pro CTSD 44 kDa) and mature (mature CTSD) forms of cathepsin D are shown. Tubulin was used as a control of equal loading. (**B**) Quantification of cathepsin-D expression (relative to tubulin) from four different western blot experiments. Results are expressed as percentage of the total cellular content of cathepsin D.

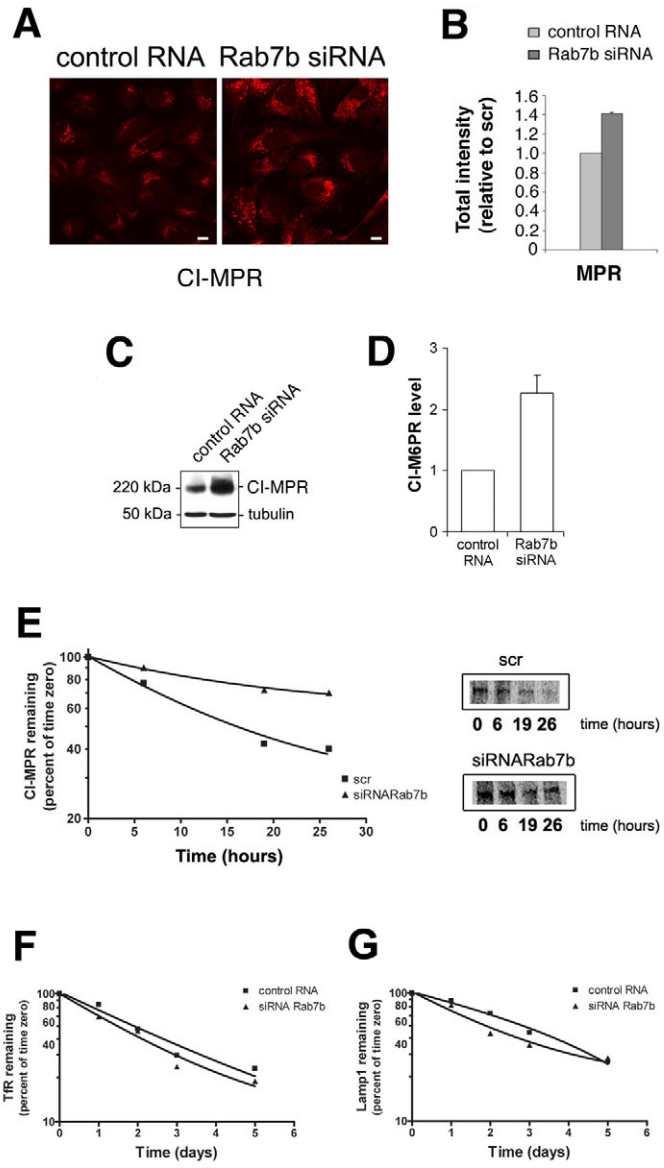

Fig. 7. Rab7b depletion alters CI-MPR trafficking. (**A**) HeLa cells treated with control RNA or with *Rab7b* siRNA were subjected to immunofluorescence analysis using CI-MPR and Cy3-conjugated secondary antibody. Scale bars: 10 µm. (**B**) Quantification of the expression levels of CI-MPR in HeLa cells treated with control RNA or siRNA against *Rab7b* was made by quantitative confocal microscopy. (**C**) HeLa cells treated with control RNA or with *Rab7b* siRNA were subjected to western blot analysis using antibodies against CI-MPR and tubulin. (**D**) Quantification of CI-MPR expression (relative to tubulin) from three different western blot experiments. (**E-G**) HeLa cells treated with control RNA or with *Rab7b* siRNA were labelled with [^{35}S]methionine/cysteine and chased for the indicated times. Equal amounts of cells were harvested (as determined by protein assay) and lysed. CI-MPR (E), TfR (F) or Lamp1 (G) was immunoprecipitated, and subjected to SDS-PAGE and autoradiography. Quantification of three independent experiments is plotted on a semi-log plot.

for 90 minutes and chased in complete medium for 3 hours to allow receptors to fold and transit through the Golgi (Sahagian and Neufeld, 1983). This time point was considered time 0 and, subsequently, the receptor turnover was measured. At time 0, the amount of newly synthesized CI-MPR was increased in Rab7b-depleted cells and, in addition, at later time points we observed that CI-MPR was more rapidly degraded in control cells compared with Rab7b-depleted cells (Fig. 7E).

In order to establish whether the effect was specific for this receptor, we also analyzed synthesis and turnover of other transmembrane proteins such as the transferrin receptor (TfR) and the lysosomal membrane protein Lamp1. TfR is normally internalized after binding of transferrin-Fe^{3+} by endocytosis and recycled back to the plasma membrane after releasing of the ligand (Yamashiro and Maxfield, 1984). Lamp1 is a type I transmembrane protein with a short cytoplasmic tail (11 amino acids); this tail is responsible for the sorting of the protein from TGN to late endosomes and/or lysosomes (Braulke and Bonifacino, 2009). The analysis of TfR and Lamp1 turnover showed that there was no difference in the kinetics of TfR or Lamp1 between control cells and cells depleted of Rab7b (Fig. 7F,G). Therefore, our findings are consistent with the hypothesis that Rab7b is indispensable specifically for the CI-MPR sorting pathway.

CI-MPR is missorted in cells lacking Rab7b

Rab7b-depleted cells showed an increased level of CI-MPR (Fig. 7). We assumed that, in these cells, the receptor accumulated in some compartment. To test this, the localization of CI-MPR was quantified by confocal quantitative analysis in control and Rab7b-depleted cells using several markers of Golgi and early and late endosomes. In control cells, 20% of the CI-MPR colocalized with TGN46, about 25% with giantin and 15% with EEA-1, as shown in Fig. 8.

In cells depleted of Rab7b, CI-MPR localization was altered: about 35% of CI-MPR-positive vesicles were TGN46 positive, whereas only 10% of the receptor was localized to giantin-positive Golgi structures. Therefore, in cells lacking Rab7b, CI-MPR accumulated in vesicles containing TGN46. These structures were not early or late endosomes, because CI-MPR did not accumulate in structure positives for the early endosomal marker EEA-1 (Fig. 8), or the late endosomal markers Lamp1, LBPA or Rab7 (data not shown).

In addition, CI-MPR distribution was altered in cells depleted for Rab7b (Fig. 9). In control cells, CI-MPR was clustered in the perinuclear area (late endosomes and TGN), whereas, in cells treated with siRNA against *Rab7b*, CI-MPR was more dispersed. We quantified the distribution of the receptor, calculating its intensity in concentric rings centred in the perinuclear area. As shown in Fig. 9, there was a clear difference in the CI-MPR distribution in cells depleted for Rab7b compared with control cells. We performed the same analysis for TGN46 and obtained similar results as for CI-MPR (Fig. 9). These results confirm that Rab7b plays an important role in the trafficking of MPRs and TGN46, as they both need Rab7b for proper intracellular localization.

Depletion of Rab7b increases AP-3 levels without affecting its distribution

Adaptor proteins are multiprotein complexes involved in cargo sorting through binding to signals present in the cytoplasmic tails of cargo proteins. AP-1 is located on the TGN and contributes to the sorting of CI-MPR and its cargo hydrolases. AP-3 mediates selective transport to lysosomes (Chapuy et al., 2008). The lysosomal membrane proteins LimpII and Lamp1 were the first cargo proteins shown to bind to AP-3 (Le Borgne et al., 1998).

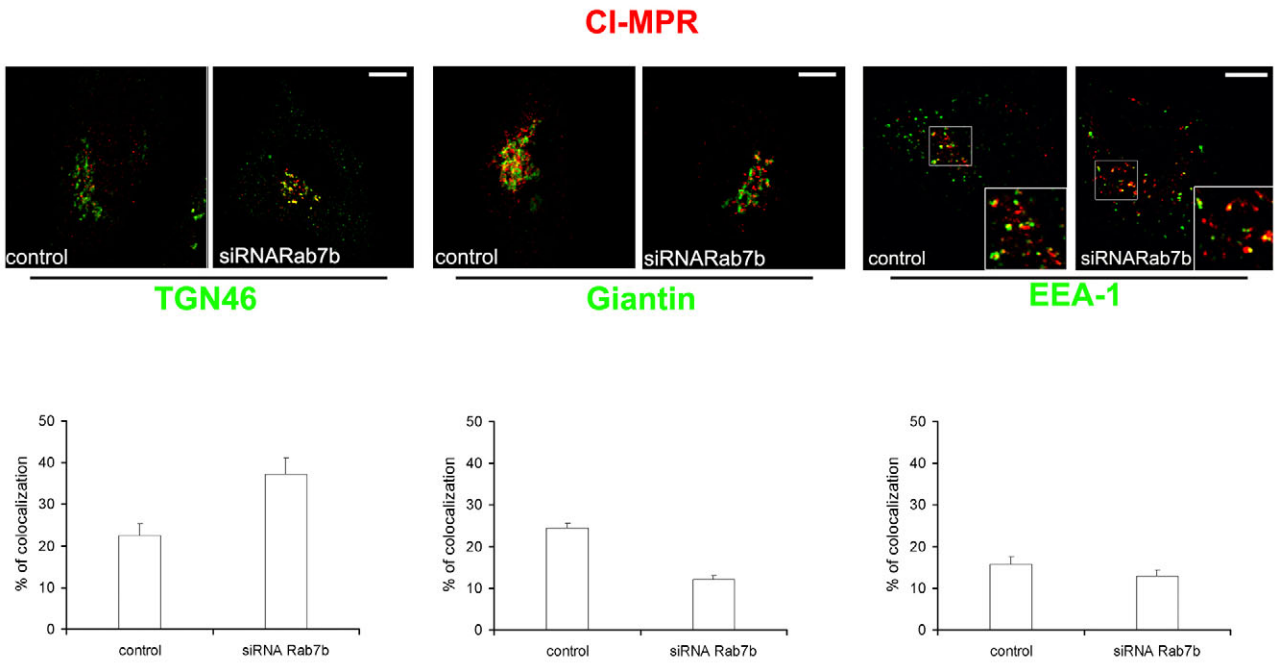

Fig. 8. Depletion of Rab7b causes CI-MPR missorting. HeLa cells treated with control RNA or siRNA against *Rab7b* were permeabilized before fixation and stained, as indicated, with antibody against CI-MPR in combination with a Cy3-conjugated secondary antibody together with antibodies against TGN46, giantin or EEA-1 in combination with an FITC-conjugated secondary antibody. Bar graphs show the percentage of colocalization of CI-MPR with TGN46, giantin or EEA-1 in Rab7b-depleted cells compared with control cells. The graphs represent the average (± s.e.) of three individual experiments in which at least 50 cells were quantified per experiment. Quantification of colocalization was determined by Zeiss LSM 510 software (version 3.2).

In order to understand how Rab7b could regulate the trafficking between late endosomes and the TGN, we examined AP-1 and AP-3 localization in cells depleted of Rab7b. We stained for AP-1 or AP-3 using specific antibodies against anti-adaptin-γ and anti-adaptin-δ, respectively (Fig. 10A). Microscopic analysis of AP-1 and AP-3 distribution showed a very similar distribution between control cells and Rab7b-depleted cells. The only apparent difference was an increased AP-3 intensity in the Rab7b-depleted cells. The increase in AP-3 was also confirmed by western blotting (Fig. 10B). AP-3 has been thought to be involved in the transport in the latter part of the endocytic pathway (Peden et al., 2004) but also at the TGN (Gupta et al., 2006). We found no effect on the half-life of Lamp1 (Fig. 7), whereas transport of CI-MPR was altered by Rab7 depletion. At this stage, it is not possible to draw any conclusion from the finding that AP-3 is elevated, but it is an interesting observation that could lead to a more mechanistic understanding of the processes involved in Rab-mediated transport linked to the level of adaptor synthesis.

Depletion of Rab7b by RNAi perturbs retrograde transport of cholera toxin B-subunit to the Golgi

To examine whether Rab7b regulates the transport from endosomes to the Golgi, we followed the trafficking of cholera toxin fragment B (CTxB) by using an immunofluorescence-based toxin-uptake assay (Fig. 11). Fluorescent-conjugated CTxB was internalized for 30 minutes in control cells and in cells depleted of Rab7b, and transport of CTxB to the Golgi was assessed. Efficiency of transport to the Golgi was monitored microscopically after sample fixation. In control cells, CTxB traffics through the endocytic pathway towards the Golgi, showing enrichment in the perinuclear region (Fig. 11A). However, in Rab7b-depleted cells, CTxB was not able to reach the Golgi, remaining predominantly associated with more peripheral structures (Fig. 11A). Quantitative analysis showed that Rab7b depletion strongly inhibits (by about 50%) CTxB transport towards the Golgi region (Fig. 11B). This result indicates that the absence of Rab7b prevents cholera toxin from reaching the Golgi, thus confirming that Rab7b is involved in the traffic from endosomes to the Golgi.

Discussion

Rab proteins are small GTPases involved in the regulation of membrane trafficking

Rab7b is a recently identified small GTPase of the Rab family and has a high similarity to Rab7 (Wang et al., 2007; Yang et al., 2004). Rab7b has been reported to be specifically expressed in CD14-positive cells in peripheral blood and, similarly to Rab7, to be involved in the regulation of transport to degradative compartments in the endocytic pathway (Wang et al., 2007; Yang et al., 2004).

It has been proposed that isoforms of Rab proteins should be at least 70% identical, and also show conservation of the RabF and RabSF motifs and specific characteristics (Pereira-Leal and Seabra, 2000; Pereira-Leal and Seabra, 2001). Following these criteria, Rab7b is not a true Rab7 isoform; indeed, the identity with Rab7 is only about 50% and the RabF and RabSF motifs are not conserved. However, it clearly belongs to the VII functional group comprising Rab7 and Rab9, two related subfamilies (Mackiewicz and Wyroba, 2009). On the basis of this we decided to investigate in detail the role of Rab7b in intracellular vesicular trafficking and compare its effects to those of Rab7.

By examining Rab7b expression, we found that *Rab7b* transcripts are very abundant in monocytes, macrophages and dendritic cells, in agreement with previously published data (Yang et al., 2004). In

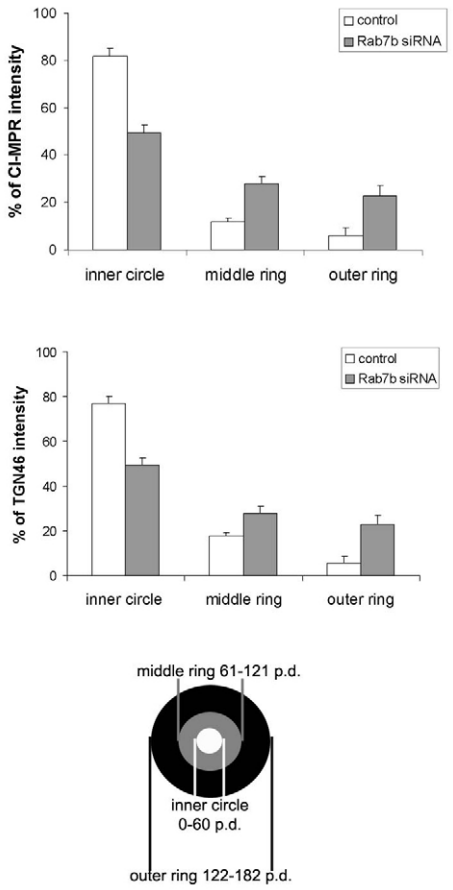

Fig. 9. Depletion of Rab7b causes dispersion of CI-MPR and TGN46. HeLa cells were treated with control RNA or siRNA against *Rab7b* and stained for CI-MPR or TGN46. Confocal images were analyzed using ImageJ, where at least 50 cells were quantified per experiment. Circles centred on the peak of fluorescent signal were drawn and the intensity of CI-MPR or TGN46 inside the circles was quantified relative to the total intensity in the whole cells. Pixel distance (p.d.) of the concentric circles is shown.

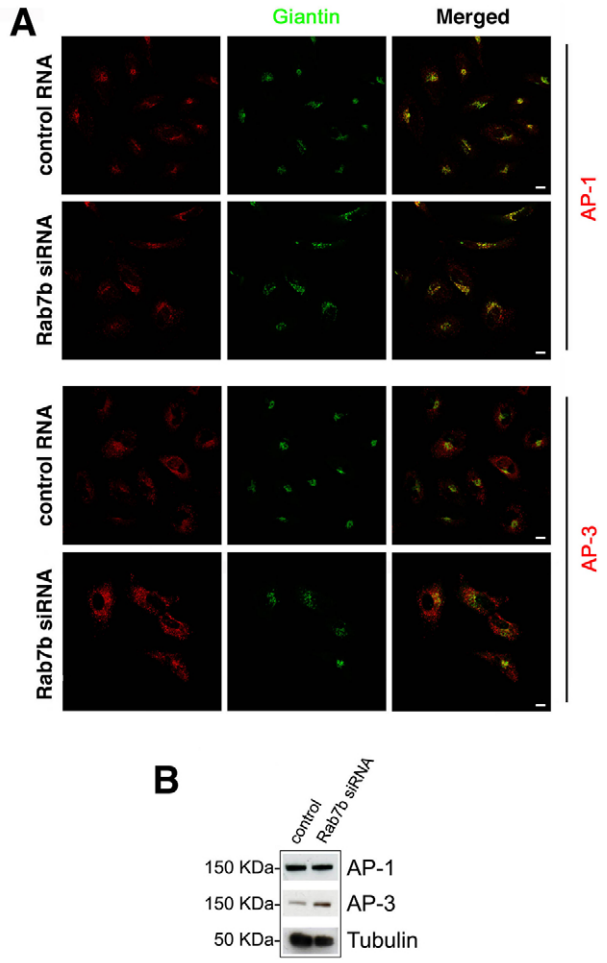

Fig. 10. Rab7b depletion and adaptor proteins. (**A**) HeLa cells treated with control RNA or with *Rab7b* siRNA were subjected to immunofluorescence analysis using anti-γ-adaptin (AP-1 complex) or anti-δ-adaptin (AP-3 complex) antibodies in combination with Cy3-conjugated secondary antibody together with anti-giantin antibody in combination with a FITC-conjugated secondary antibody. Scale bars: 10 µm. (**B**) HeLa cells treated with control RNA or with *Rab7b* siRNA were subjected to western blot analysis using antibodies against AP-1, AP-3 and tubulin.

addition, we detected *Rab7b* transcripts in HeLa cells and in other non-haemopoietic cell lines (Fig. 1; data not shown). Therefore, we conclude that Rab7b expression is not restricted to some haemopoietic cells but has a range of expression levels in different cells. Most Rab proteins are ubiquitously expressed, although cell-type- or tissue-specific Rabs have been identified. It is known that specialized cells use transport pathways that are unique for their differentiated state, requiring specific Rab proteins. Indeed, Rab17, Rab18, Rab20 and Rab25 are specific to polarized cells, whereas Rab3 is only expressed in neurons and neuroendocrine cells (Ng and Tang, 2008; van Ijzendoorn et al., 2003). Another issue is that even ubiquitously expressed Rab proteins are not expressed at the same level in the different tissues, and Rab7, for instance, has a tissue-specific pattern of expression (Verhoeven et al., 2003).

On the basis of this, it is not surprising that human Rab7b is more expressed in heart, skeletal muscle and peripheral blood leukocytes, and less expressed in some other tissues. In addition, we demonstrated here that Rab7b always has the same localization in all the cell lines used, independent of its level of expression (Fig. 2; supplementary material Fig. S1). We confirmed the localization of wild-type Rab7b on late endosomal compartments, but we also observed an additional partial colocalization with Golgi and TGN markers (Figs 2, 3; supplementary material Figs S2-S4), at variance with Rab7 (supplementary material Fig. S5). Rab7 has been shown to interact with a retromer-like complex, and it has been recently identified as a component and regulator of the retromer and to be involved in retromer recruitment to endosomes (Nakada-Tsukui et al., 2005; Rojas et al., 2008). Its localization to late endosomes, however, has been established in several studies and Rab7 is used as a marker for this part of the endosomal pathway (Chavrier et al., 1990; Harada et al., 2005). The level of colocalization between Rab7b and Golgi and/or TGN markers was higher with the constitutively active mutant Rab7b Q67L (Figs 2, 3; supplementary material Figs S2-S4). This is very different from the active Rab7 mutant (Q67L), the localization of which is restricted to late endosomes and lysosomes (supplementary material Fig. S5) (Bucci et al., 2000; Meresse et al., 1995). Colocalization

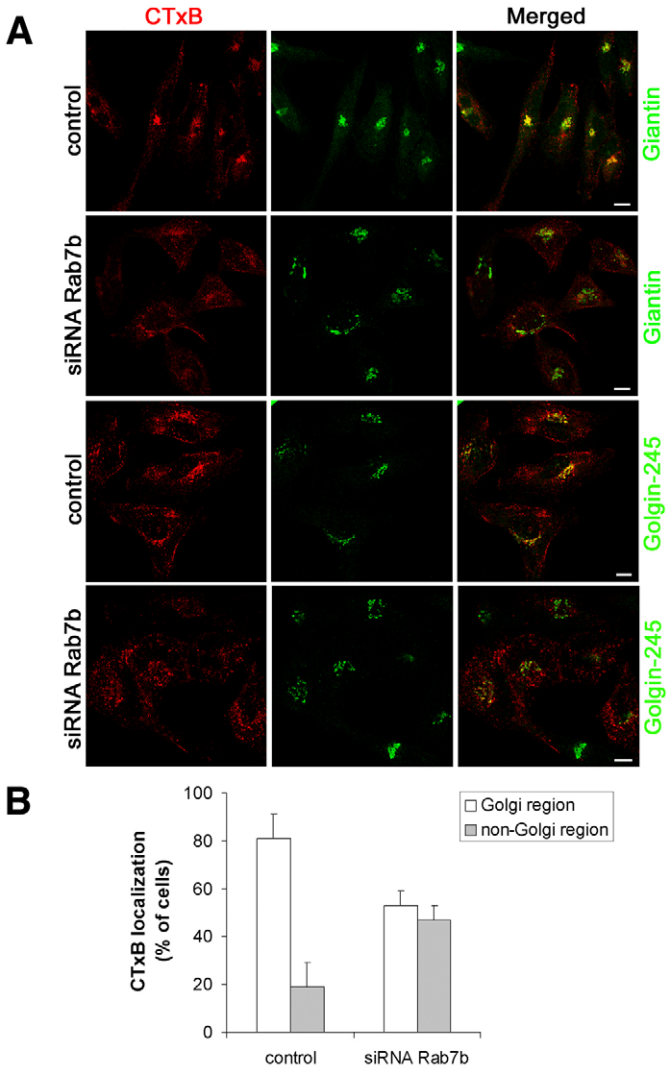

Fig. 11. Rab7b depletion inhibits retrograde transport of cholera toxin B-subunit to the Golgi. (**A**) HeLa cells treated with control RNA or with *Rab7b* siRNA were allowed to internalize fluorescent (red) cholera toxin B-subunit (CTxB) for 30 minutes. Cells were then fixed and stained with anti-giantin and anti-Golgin-245 antibodies, followed by a secondary antibody conjugated with Cy2 (green), as indicated. Scale bars: 10 µm. (**B**) Quantitative analysis of CTxB localization in the Golgi area. Quantification of colocalization was determined by Zeiss LSM 510 software (version 3.2).

of the Rab7b Q67L mutant protein with Golgi and TGN markers was detected not only in HeLa cells but also in Raw264.7, U-937 and THP-1 differentiated cells (Fig. 2; supplementary material Figs S2, S4, and data not shown). Taken together, these data lead to the conclusion that Rab7b might function at the transport steps between the Golgi and the endosomal pathway.

Other Rab proteins also function here. Rab9 is necessary for transport between late endosomes and the trans-Golgi network, being important also for lysosome biogenesis (Barbero et al., 2002; Lombardi et al., 1993; Riederer et al., 1994). Rab13 regulates membrane trafficking between the TGN and recycling endosomes (Nokes et al., 2008), whereas Rab14 controls transport between the Golgi and early endosomes (probably both sorting and recycling) (Junutula et al., 2004). Rab34 acts at the Golgi, being required for intra-Golgi transport, but it has also been implicated in repositioning lysosomes to the juxtanuclear region (Goldenberg et al., 2007; Wang and Hong, 2002). Rab39 is clearly a Golgi-associated Rab protein, but its overexpression in HeLa cells causes a marked increase of fluid-phase endocytosis (Chen et al., 2003).

Silencing of Rab7b or expression of a Rab7b dominant-negative mutant (Rab7b T22N) causes increased hexosaminidase secretion (Fig. 5) and impaired cathepsin-D maturation (Fig. 6). These data indicate that transport of lysosomal enzymes from the TGN to endosomes is impaired in Rab7b-silenced cells. Indeed, cathepsin-D matures in acidic compartments and the accumulation of immature forms indicates that this enzyme does not reach late endosomes and lysosomes. Also, increased secretion of hexosaminidase indicates an accumulation in the secretory pathway of lysosomal enzymes that cannot be delivered to endosomes and lysosomes. No alteration of VSV-G trafficking was detected in Rab7b-depleted cells and in cells expressing the Rab7b T22N mutant, demonstrating that the biosynthetic route to the plasma membrane is not affected (supplementary material Fig. S7).

In support of a role of Rab7b at the intersection between endosomes and Golgi, silencing of Rab7b or expression of a Rab7b dominant-negative mutant causes an increase of absolute cellular levels of late endosomal markers, such as CI-MPR and cathepsin-D (Figs 6, 7; data not shown). Increased expression of lysosomal enzymes and CI-MPR has been observed when CI-MPR recycling is disrupted, for example by depletion of Rab9 (Ganley et al., 2004) or overexpression of a dominant-negative Rab9 mutant (Riederer et al., 1994). In addition, Rab7b-depleted cells displayed an increase in the amount of newly synthesized CI-MPR and a reduction in the rate of its turnover (Fig. 7). Upon the loss of Rab7b, CI-MPR became more associated with TGN46-positive small vesicles and less receptors were located to the Golgi (Fig. 8). We were not able to discern the specific identity of the compartment in which CI-MPR accumulated, although we could exclude typical early and late endosomes using EEA1, Lamp1, LBPA or Rab7 as markers. Altogether, these data show that CI-MPR recycling is disrupted in Rab7b-depleted cells and indicate that Rab7b is needed for CI-MPR trafficking to accomplish efficient delivery of lysosomal enzymes.

It has been suggested that Rab7b is not expressed in the liver (Yang et al., 2004), an organ with high levels of MPRs. However, it has been demonstrated that, in patients with I-cell disease (ICD) and in mice or cell lines lacking MPRs, hepatocytes and lymphocytes (but not fibroblasts) have an alternative MPR-independent mechanism for the transport of lysosomal enzymes to their final compartment (Dittmer et al., 1999; Saftig and Klumperman, 2009). This could also explain the stronger effects that we observed after Rab7b depletion in HeLa cells compared with U937 cells.

In Rab7b-depleted cells or cells expressing a Rab7b dominant-negative mutant, the distribution of TGN46 is also altered (Figs 4, 9). TGN46 cycles between the TGN and the cell surface, returning via endosomes, and it seems to be involved in the regulation of traffic to and from the TGN (Banting and Ponnambalam, 1997). In Rab7b-depleted cells, the TGN46 is highly redistributed to small vesicles at the cell periphery and is no longer concentrated perinuclearly. However, the protein level of TGN46 remained comparable to control cells, suggesting that TGN46 was redistributed and not degraded (Fig. 4). All these findings show that, without functional Rab7b, TGN46 is not properly localized to the TGN. This raises the possibility that TGN46, and possibly

other proteins, after leaving the TGN, fail to return, causing dispersion of the TGN markers. This would explain the presence of TGN46-scattered vesicles, as we observed in cells depleted of Rab7b. Again, these data suggest a role of Rab7b in controlling cycling between endosomes and the Golgi. Finally, the data obtained with cholera toxin B-subunit further confirm that Rab7b controls transport from endosomes to the Golgi, because in Rab7b-depleted cells the internalized toxin is not able to reach the Golgi area.

Previously published data indicate that Rab7b promotes degradation of the receptor TLR4 and it has been suggested that, similarly to Rab7, Rab7b controls transport from early endosomes to late endosomes and/or lysosomes (Wang et al., 2007). However, our data indicate that Rab7b is not involved in transport along the endocytic route; indeed, expression of a Rab7b dominant-negative mutant or silencing of Rab7b in HeLa cells did not alter EGF or EGFR degradation (supplementary material Fig. S6); this is at variance with Rab7, which, together with RILP (a Rab7 effector), controls endocytic transport to degradative compartments, strongly affecting EGF and EGFR degradation (supplementary material Fig. S6) (Progida et al., 2007; Vitelli et al., 1997). Data on TLR4 degradation can be explained by considering that this receptor, unlike EGFR, is not only destined for the degradative multivesicular late endosomes but also to other compartments, such as the Golgi apparatus, from where it can recycle to the plasma membrane (Hornef et al., 2002; Husebye et al., 2006; Latz et al., 2002). Therefore, Rab7b could impair TLR4 cycling between the Golgi and endosomes and, as a consequence, it could affect the degradation and regulate the function of this receptor.

AP-1 and AP-3 mediate the sorting of cargo membrane proteins into post-Golgi and/or TGN vesicles. AP-1 mediates the sorting of CI-MPR and AP-3 mediates the transport of lysosomal membrane proteins such as LimpII and Lamp1 (Chapuy et al., 2008). Whereas AP-1 distribution and protein level was not altered in cells depleted for Rab7b, AP-3 levels increased (Fig. 10). This suggests that the increase in AP-3 levels is a response to balance the alteration in the recycling pathway to the TGN due to the loss of Rab7b. No alteration was detected for AP-1, which is known to regulate CI-MPR transport (Le Borgne and Hoflack, 1997), showing that AP-1 is regulated differently from AP-3.

In conclusion, our results show that the major function of Rab7b is to mediate transport from endosomes to the TGN and/or Golgi, a step that is also needed to accomplish efficient delivery of lysosomal enzymes to the endocytic route.

Materials and Methods

Reagents and antibodies

Restriction and modification enzymes were from Biolabs, chemicals were from Sigma-Aldrich (St Louis, MO) and radiochemicals were from Perkin Elmer (Waltham, MA). Rhodamine-conjugated EGF was from Molecular Probes (Eugene, OR). Anti-giantin, anti-CI-MPR and anti-Rab9 were obtained from Abcam (Cambridge, UK); anti-Rab7b was from Abnova Corporation (Taipei, Taiwan); anti-Rab7, anti-adaptin-γ and anti-tubulin were from Sigma-Aldrich; anti-p230, anti-EEA-1 and anti-adaptin-δ were from Becton Dickinson Biosciences (Milano, Italy); anti-TGN46 was from AbD Serotec (Oxford, UK); anti-TfR was from Boehringer Mannheim (Ingelheim, Germany); anti-Lamp1 was from Developmental Studies Hybridoma Bank (University of Iowa, IA); anti-cathepsin-D was from Santa Cruz Biotechnology (Santa Cruz, CA); and anti-EGFR was from Fitzgerald (Concord, MA). Cy2- and Cy3-labeled secondary antibodies were purchased from Amersham Pharmacia Biotech (Uppsala, Sweden).

cDNA cloning and plasmid construction

The human *Rab7b* cDNA and the *YFP-VSV-G* plasmid were a kind gift of Xue Cao (Zhejiang University, China) and of Susanne Pfeffer (Stanford University, CA), respectively.

pEGFP-Rab7b was constructed in the following way: the coding sequence of human Rab7b was amplified by PCR using the following primers containing an *Eco*RI and a *Sal*I restriction site, respectively: Rab7b_for 5′-GGAATTCCATGAATCCCCGGAAGAAG-3′ and Rab7b_rev 5′-CCGCTCGAGTCGACTCAGCAGCATCTGCTCC-3′. The fragment was then subcloned, in frame with EGFP, into pEGFPC1 and pGadGH plasmid that was cut with *Eco*RI and *Sal*I. *Rab7b* mutants were constructed by PCR-mediated mutagenesis. The oligonucleotides used in the first amplification for *Rab7b T22N* and *Rab7b Q67L* were: T22N_rev 5′-ATTGGTGAAGGAGGGAGTTCTTTCCCACACCAATG-3′, Q67L_rev 5′-TGGAGCGGAACCGCTCCAGACCGCCCGTGTCCCAG-3′ together with pEGFP_for 5′-GATCACTCTCGGCATGGAC-3′. In the second amplification, the two PCR products were used as primers together with Rab7b_rev. The mutated cDNAs were then cloned into pEGFPC1 vector and the constructs were sequenced to exclude the presence of unwanted mutations caused by the *Taq* polymerase. The pcDNA-2×HA-Rab7b wild-type and mutants were obtained by PCR amplification with the following primers containing an *Eco*RI and a *Sal*I restriction site, respectively: 5′-ATGGAATTCTTATGAATCCCCGGAAGAAGGTG-3′ and Rab7b_rev. The fragment was then subcloned into pcDNA-2×HA plasmid, which contains the HA epitope repeated twice.

Cell culture, transfections and siRNA oligonucleotides

HeLa and RAW 264.7 cells were grown in Dulbecco's modified Eagle's medium (DMEM) supplemented with 10% fetal calf serum (FCS), 2 mM glutamine, 100 U/ml penicillin and 100 μg/ml streptomycin; U-937 and THP-1 cells were grown in RPMI 1640 with 10% FCS, 2 mM glutamine, 100 U/ml penicillin and 100 μg/ml streptomycin. Monocyte-derived dendritic cells were kindly provided by Ole J. Landsverk and Anett H. Ottesen (University of Oslo, Norway).

Transfection was performed using Metafectene Pro from Biontex (Martinsried, Germany) as indicated by the manufacturer.

For RNA interference (RNAi), the following oligonucleotides were used: siRNA-Rab7b, sense sequence 5′-GUAGCUCAAGGCUGGUGUATT-3′ and antisense sequence 5′-UACACCAGCCUUGAGCUACTT-3′; siRNA-Rab7, sense sequence 5′-GGAUGACCUCUAGGAAGAATT-3′ and antisense sequence 5′-UUCUUCCUAGAGGUCAUCCTT-3′. As negative control a scrambled sequence was used: sense scrambled control 5′-ACUUCGAGCGUGCAUGGCUTT-3′ and antisense scrambled control 5′-AGCCAUGCACGCUCGAAGUTT-3′. All chemically synthesized oligonucleotides were purchased from Eurofins MWG Operon (Ebersberg, Germany).

Transfection of HeLa cells with siRNA was performed as described (Progida et al., 2007). Briefly, HeLa cells were plated 1 day before transfection in 6-cm dishes (~4×10^5 cells/dish). Cells were transfected with siRNA using Oligofectamine (Invitrogen, Carlsbad, CA) for 72 hours, replated and left for another 48 hours before further experiments were carried out. Transfection of U937 and dendritic cells was performed using an Amaxa Nucleofector device, according to the manufacturer's instruction.

Standard RNA procedures

Total RNA was extracted from cells with the RNeasy mini kit according to the manufacturer's instructions (Qiagen). Mixtures (12 μl) containing 5 μg cytosolic RNA, 0.9 mM deoxyribonucleotide triphosphate and 50 ng of random hexamers were heated at 65°C and immediately cooled on ice. First-strand cDNA synthesis was then carried out with 5 U/μl Superscript RT (Invitrogen) in the presence of 0.01 M DTT and 2 U/μl ribonuclease inhibitor at 37°C for 50 minutes. Reactions were stopped by heat inactivation at 70°C for 15 minutes.

Quantitative real-time PCR

Primers for *Rab7b* (forward primer, 5′-GGCCAGCATCCTCTCCAAGATTATC-3′; reverse primer; 5′-GATGCAGCCATCGGAGCCCTTGT-3′), and human actin (forward primer; 5′-CTGACTGACTACCTCATGAAGATCCT-3′, reverse primer; 5′-CTTAATGTCACGCACGATTTCC-3′) were purchased from Eurofin MWG Operon. Quantitative real-time PCRs were performed using SYBR Green JumpStart ReadyMix (Sigma) in the Smart Cycler II Real-Time PCR detection system (Cepheid). The PCR programme was as follows: 1 cycle 3 minutes at 94°C; 35 cycles 30 seconds at 94°C, 30 seconds at 60°C, 30 seconds at 72°C; 1 cycle 6 seconds at 75°C. The specificity of the PCR product was checked by performing a melting-curve test.

EGF and EGFR degradation assay

For EGF degradation, cells grown on coverslips were serum-starved overnight in starvation medium (DMEM supplemented with 20 mM HEPES, pH 7.3, and 0.5% BSA). Internalization and degradation of EGF was performed as described (Spinosa et al., 2008). For the EGFR-degradation assay, HeLa cells were treated with 10 μg/ml cycloheximide for 1 hour and then stimulated with 50 ng/ml EGF for 15, 60, 120 or 180 minutes. The levels of non-degraded EGFR were determined by western blotting as described (Progida et al., 2007).

Confocal fluorescence microscopy

HeLa cells grown on coverslips were washed once with phosphate-buffered saline (PBS), permeabilized with 0.1% saponin and fixed with 3% paraformaldehyde. Incubation with primary antibodies was for 20 minutes at room temperature. After

washes in 0.25% saponin, cells were incubated with the appropriate secondary antibodies for 20 minutes in the dark, at room temperature. In some experiments, cells were treated for different time points with brefeldin A (1 μg/ml) before fixation. Mounted coverslips were examined using a Zeiss LSM 510 Meta confocal microscope. Intensities were quantified using the Zeiss LSM 510 software (version 3.2). Confocal pictures used for quantification were scanned at the same pinhole, offset gain and amplifier values below pixel saturation. Image processing was carried out with Adobe Photoshop version 7.0.

VSV-G secretion assay

Cells grown on coverslips were transfected with YFP–VSV-G. At 2 hours after transfection, cells were shifted to 39°C for 16 hours. To release VSV-G, cells were transferred to 32°C and the samples were fixed at the indicated times.

Hexosaminidase secretion assay

Cells grown in 6-cm dishes were washed twice with TD buffer (0.137 M NaCl, 5 mM KCl, 0.7 mM Na_2PO_4 and 25 mM Tris-HCl, pH 7.4) and incubated for 8 hours at 37°C with 1 ml of pre-warmed DMEM without phenol red plus 10 mM M6P. Secreted hexosaminidase activity and intracellular hexosaminidase levels were measured as described (Riederer et al., 1994).

CI-M6PR, TfR and Lamp1 half-lives

After RNA treatment, cells were seeded into six-well plates. The following day, cells were washed twice with TD buffer (0.137 M NaCl, 5 mM KCl, 0.7 mM Na_2PO_4 and 25 mM Tris-HCl, pH 7.4) and incubated for 30 minutes at 37°C in medium lacking methionine and cysteine. Cells were labelled with [^{35}S]methionine and cysteine (100 μCi/ml) for 90 minutes at 37°C, washed twice with medium containing methionine, cysteine and 7.5% dialyzed FBS, and chased in the same medium for up to 5 days. At the indicated times, cells were washed twice with cold PBS and lysed in RIPA buffer containing protease inhibitors for 10 minutes. After centrifugation at 100,000 ***g*** for 10 minutes at 4°C, the supernatant was immunoprecipitated with anti-CI-M6PR, anti-TfR or anti-Lamp1 antibodies. Samples were then subjected to SDS-PAGE and autoradiography and analyzed by Phosphorimager for quantification.

Cholera-toxin uptake

Cholera-toxin uptake was performed as described previously (Ganley et al., 2008). Briefly, HeLa cells grown on coverslips were incubated with 4 μg/ml cholera toxin B-subunit conjugated to Alexa Fluor 594 (Invitrogen) for 30 minutes at 37°C, then washed and subsequently chased for 30 minutes at 37°C. After incubation, cells were fixed with 3% paraformaldehyde and stained for immunofluorescence.

We are extremely grateful to Suzanne Pfeffer (Stanford University, CA) for helpful suggestions with several of the experiments and for critical reading of the manuscript. We thank Xue Cao (Zhejiang University, China) for the kind gift of *Rab7b* cDNA and Mary McCaffrey for critical reading of the manuscript. The financial support of AIRC (Associazione Italiana per la Ricerca sul Cancro, Grant no. 4496 of 2007 to C.B.), of Telethon-Italy (Grant no. GGP09045 to C.B.), of the the Norwegian Research Council (grant to O.B.) and of EU (Grant Microban EU network no MRTN-CT-2003-504227 to C.P.) is gratefully acknowledged.

Supplementary material available online at
http://jcs.biologists.org/cgi/content/full/123/9/1480/DC1

References

Banting, G. and Ponnambalam, S. (1997). TGN38 and its orthologues: roles in post-TGN vesicle formation and maintenance of TGN morphology. *Biochim. Biophys. Acta* **1355**, 209-217.

Barbero, P., Bittova, L. and Pfeffer, S. R. (2002). Visualization of Rab9-mediated vesicle transport from endosomes to the trans-Golgi in living cells. *J. Cell Biol.* **156**, 511-518.

Braulke, T. and Bonifacino, J. S. (2009). Sorting of lysosomal proteins. *Biochim. Biophys. Acta* **1793**, 605-614.

Bucci, C., Chiariello, M., Lattero, D., Maiorano, M. and Bruni, C. B. (1999). Interaction cloning and characterization of the cDNA encoding the human prenylated rab acceptor (PRA1). *Biochem. Biophys. Res. Commun.* **258**, 657-662.

Bucci, C., Thomsen, P., Nicoziani, P., McCarthy, J. and van Deurs, B. (2000). Rab7: a key to lysosome biogenesis. *Mol. Biol. Cell* **11**, 467-480.

Cai, H., Reinisch, K. and Ferro-Novick, S. (2007). Coats, tethers, Rabs, and SNAREs work together to mediate the intracellular destination of a transport vesicle. *Dev. Cell* **12**, 671-682.

Cantalupo, G., Alifano, P., Roberti, V., Bruni, C. B. and Bucci, C. (2001). Rab-interacting lysosomal protein (RILP): the Rab7 effector required for transport to lysosomes. *EMBO J.* **20**, 683-693.

Ceresa, B. P. (2006). Regulation of EGFR endocytic trafficking by rab proteins. *Histol. Histopathol.* **21**, 987-993.

Ceresa, B. P. and Bahr, S. J. (2006). Rab7 activity affects epidermal growth factor:epidermal growth factor receptor degradation by regulating endocytic trafficking from the late endosome. *J. Biol. Chem.* **281**, 1099-1106.

Chapuy, B., Tikkanen, R., Mühlhausen, C., Wenzel, D., von Figura, K. and Höning, S. (2008). AP-1 and AP-3 mediate sorting of melanosomal and lysosomal membrane proteins into distinct post-Golgi trafficking pathways. *Traffic* **9**, 1157-1172.

Chavrier, P., Parton, R. G., Hauri, H. P., Simons, K. and Zerial, M. (1990). Localization of low molecular weight GTP binding proteins to exocytic and endocytic compartments. *Cell* **62**, 317-329.

Chen, T., Han, Y., Yang, M., Zhang, W., Li, N., Wan, T., Guo, J. and Cao, X. (2003). Rab39, a novel Golgi-associated Rab GTPase from human dendritic cells involved in cellular endocytosis. *Biochem. Biophys. Res. Commun.* **303**, 1114-1120.

Deinhardt, K., Salinas, S., Verastegui, C., Watson, R., Worth, D., Hanrahan, S., Bucci, C. and Schiavo, G. (2006). Rab5 and Rab7 control endocytic sorting along the axonal retrograde transport pathway. *Neuron* **52**, 293-305.

Dittmer, F., Ulbrich, E. J., Hafner, A., Schmahl, W., Meister, T., Pohlmann, R. and von Figura, K. (1999). Alternative mechanisms for trafficking of lysosomal enzymes in mannose 6-phosphate receptor-deficient mice are cell type-specific. *J. Cell Sci.* **112**, 1591-1597.

Dong, J., Chen, W., Welford, A. and Wandinger-Ness, A. (2004). The proteasome alpha-subunit XAPC7 interacts specifically with Rab7 and late endosomes. *J. Biol. Chem.* **279**, 21334-21342.

Ganley, I. G., Carroll, K., Bittova, L. and Pfeffer, S. (2004). Rab9 GTPase regulates late endosome size and requires effector interaction for its stability. *Mol. Biol. Cell* **15**, 5420-5430.

Ganley, I. G., Espinosa, E. and Pfeffer, S. R. (2008). A syntaxin 10-SNARE complex distinguishes two distinct transport routes from endosomes to the trans-Golgi in human cells. *J. Cell Biol.* **180**, 159-172.

Goldenberg, N. M., Grinstein, S. and Silverman, M. (2007). Golgi-bound Rab34 is a novel member of the secretory pathway. *Mol. Biol. Cell* **18**, 4762-4771.

Grosshans, B. L., Ortiz, D. and Novick, P. (2006). Rabs and their effectors: achieving specificity in membrane traffic. *Proc. Natl. Acad. Sci. USA* **103**, 11821-11827.

Gupta, S. N., Kloster, M. M., Rodionov, D. G. and Bakke, O. (2006). Re-routing of the invariant chain to the direct sorting pathway by introduction of an AP3-binding motif from LIMP II. *Eur J. Cell Biol.* **85**, 457-467.

Gutierrez, M., Munafó, D., Berón, W. and Colombo, M. (2004). Rab7 is required for the normal progression of the autophagic pathway in mammalian cells. *J. Cell Sci.* **117**, 2687-2697.

Harada, M., Kawaguchi, T., Kumemura, H., Terada, K., Ninomiya, H., Taniguchi, E., Hanada, S., Baba, S., Maeyama, M., Koga, H. et al. (2005). The Wilson disease protein ATP7B resides in the late endosomes with Rab7 and the Niemann-Pick C1 protein. *Am. J. Pathol.* **166**, 499-510.

Harrison, R., Bucci, C., Vieira, O., Schroer, T. and Grinstein, S. (2003). Phagosomes fuse with late endosomes and/or lysosomes by extension of membrane protrusions along microtubules: role of Rab7 and RILP. *Mol. Cell. Biol.* **23**, 6494-6506.

Hornef, M. W., Frisan, T., Vandewalle, A., Normark, S. and Richter-Dahlfors, A. (2002). Toll-like receptor 4 resides in the Golgi apparatus and colocalizes with internalized lipopolysaccharide in intestinal epithelial cells. *J. Exp. Med.* **195**, 559-570.

Husebye, H., Halaas, Ø., Stenmark, H., Tunheim, G., Sandanger, Ø., Bogen, B., Brech, A., Latz, E. and Espevik, T. (2006). Endocytic pathways regulate Toll-like receptor 4 signaling and link innate and adaptive immunity. *EMBO J.* **25**, 683-692.

Jager, S., Bucci, C., Tanida, I., Ueno, T., Kominami, E., Saftig, P. and Eskelinen, E. L. (2004). Role for Rab7 in maturation of late autophagic vacuoles. *J. Cell Sci.* **117**, 4837-4848.

Johansson, M., Lehto, M., Tanhuanpaa, K., Cover, T. L. and Olkkonen, V. M. (2005). The Oxysterol-binding protein homologue ORP1L interacts with Rab7 and alters functional properties of late endocytic compartments. *Mol. Biol. Cell* **16**, 5480-5492.

Junutula, J. R., De Maziére, A. M., Peden, A. A., Ervin, K. E., Advani, R. J., van Dijk, S. M., Klumperman, J. and Scheller, R. H. (2004). Rab14 is involved in membrane trafficking between the Golgi complex and endosomes. *Mol. Biol. Cell* **15**, 2218-2229.

Latz, E., Visintin, A., Lien, E., Fitzgerald, K. A., Monks, B. G., Kurt-Jones, E. A., Golenbock, D. T. and Espevik, T. (2002). Lipopolysaccharide rapidly traffics to and from the Golgi apparatus with the toll-like receptor 4-MD-2-CD14 complex in a process that is distinct from the initiation of signal transduction. *J. Biol. Chem.* **277**, 47834-47843.

Le Borgne, R. and Hoflack, B. (1997). Mannose 6-phosphate receptors regulate the formation of clathrin-coated vesicles in the TGN. *J. Cell Biol.* **137**, 335-345.

Le Borgne, R., Alconada, A., Bauer, U. and Hoflack, B. (1998). The mammalian AP-3 adaptor-like complex mediates the intracellular transport of lysosomal membrane glycoproteins. *J. Biol. Chem.* **273**, 29451-29461.

Lombardi, D., Soldati, T., Riederer, M. A., Goda, Y., Zerial, M. and Pfeffer, S. R. (1993). Rab9 functions in transport between late endosomes and the trans Golgi network. *EMBO J.* **12**, 677-682.

Mackiewicz, P. and Wyroba, E. (2009). Phylogeny and evolution of Rab7 and Rab9 proteins. *BMC Evol. Biol.* **9**, 101.

Markgraf, D. F., Peplowska, K. and Ungermann, C. (2007). Rab cascades and tethering factors in the endomembrane system. *FEBS Lett.* **581**, 2125-2130.

Meresse, S., Gorvel, G. P. and Chavrier, P. (1995). The rab7 GTPase resides on a vesicular compartment connected to lysosomes. *J. Cell Sci.* **108**, 3349-3358.

Mizuno, K., Kitamura, A. and Sasaki, T. (2003). Rabring7, a novel Rab7 target protein with a RING finger motif. *Mol. Biol. Cell* **14**, 3741-3752.

Moore, I., Schell, J. and Palme, K. (1995). Subclass-specific sequence motifs identified in Rab GTPases. *Trends Biochem. Sci.* **20**, 10-12.

Nakada-Tsukui, K., Saito-Nakano, Y., Ali, V. and Nozaki, T. (2005). A retromerlike complex is a novel Rab7 effector that is involved in the transport of the virulence factor cysteine protease in the enteric protozoan parasite Entamoeba histolytica. *Mol. Biol. Cell* **16**, 5294-5303.

Ng, E. L. and Tang, B. L. (2008). Rab GTPases and their roles in brain neurons and glia. *Brain Res. Rev.* **58**, 236-246.

Nokes, R. L., Fields, I. C., Collins, R. N. and Fölsch, H. (2008). Rab13 regulates membrane trafficking between TGN and recycling endosomes in polarized epithelial cells. *J. Cell Biol.* **182**, 845-853.

Peden, A. A., Oorschot, V., Hesser, B. A., Austin, C. D., Scheller, R. H. and Klumperman, J. (2004). Localization of the AP-3 adaptor complex defines a novel endosomal exit site for lysosomal membrane proteins. *J. Biol. Chem.* **7**, 1065-1076.

Pereira-Leal, J. B. and Seabra, M. C. (2000). The mammalian Rab family of small GTPases: definition of family and subfamily sequence motifs suggests a mechanism for functional specificity in the Ras superfamily. *J. Mol Biol.* **301**, 1077-1087.

Pereira-Leal, J. B. and Seabra, M. C. (2001). Evolution of the Rab family of small GTP-binding proteins. *J. Mol Biol.* **313**, 889-901.

Pereira-Leal, J. B., Hume, A. N. and Seabra, M. C. (2001). Prenylation of Rab GTPases: molecular mechanisms and involvement in genetic disease. *FEBS Lett.* **498**, 197-200.

Pfeffer, S. R. (2005a). A model for Rab GTPase localization. *Biochem. Soc. Trans.* **33**, 627-630.

Pfeffer, S. R. (2005b). Structural clues to Rab GTPase functional diversity. *J. Biol. Chem.* **280**, 15485-15488.

Press, B., Feng, Y., Hoflack, B. and Wandinger-Ness, A. (1998). Mutant Rab7 causes the accumulation of cathepsin D and cation-independent mannose 6-phosphate receptor in an early endocytic compartment. *J. Cell Biol.* **140**, 1075-1089.

Progida, C., Malerød, L., Stuffers, S., Brech, A., Bucci, C. and Stenmark, H. (2007). RILP is required for proper morphology and function of late endosomes. *J. Cell Sci.* **120**, 3729-3737.

Riederer, M. A., Soldati, T., Shapiro, A. D., Lin, J. and Pfeffer, S. R. (1994). Lysosome biogenesis requires Rab9 function and receptor recycling from endosomes to the trans-Golgi network. *J. Cell Biol.* **125**, 573-582.

Rojas, R., van Vlijmen, T., Mardones, G. A., Prabhu, Y., Rojas, A. L., Mohammed, S., Heck, A. J., Raposo, G., van der Sluijs, P. and Bonifacino, J. S. (2008). Regulation of retromer recruitment to endosomes by sequential action of Rab5 and Rab7. *J. Cell Biol.* **183**, 513-526.

Saftig, P. and Klumperman, J. (2009). Lysosome biogenesis and lysosomal membrane proteins: trafficking meets function. *Nat. Rev. Mol. Cell Biol.* **10**, 623-635.

Sahagian, G. G. and Neufeld, E. F. (1983). Biosynthesis and turnover of the mannose 6-phosphate receptor in cultured Chinese hamster ovary cells. *J. Biol. Chem.* **258**, 7121-7128.

Sakane, A., Hatakeyama, S. and Sasaki, T. (2007). Involvement of Rabring7 in EGF receptor degradation as an E3 ligase. *Biochem. Biophys. Res. Commun.* **357**, 1058-1064.

Saxena, S., Bucci, C., Weis, J. and Kruttgen, A. (2005). The small GTPase Rab7 controls the endosomal trafficking and neuritogenic signaling of the nerve growth factor receptor TrkA. *J. Neurosci.* **25**, 10930-10940.

Seabra, M. C. and Wasmeier, C. (2004). Controlling the location and activation of Rab GTPases. *Curr. Opin. Cell Biol.* **16**, 451-457.

Spinosa, M. R., Progida, C., De Luca, A., Colucci, A. M. R., Alifano, P. and Bucci, C. (2008). Functional characterization of Rab7 mutant proteins associated with Charcot-Marie-Tooth type 2B disease. *J. Neurosci.* **28**, 1640-1648.

Stein, M. P., Feng, Y., Cooper, K. L., Welford, A. M. and Wandinger-Ness, A. (2003). Human VPS34 and p150 are Rab7 interacting partners. *Traffic* **4**, 754-771.

Sun, Y., Buki, K. G., Ettala, O., Vaaraniemi, J. P. and Vaananen, H. K. (2005). Possible role of direct Rac1-Rab7 interaction in ruffled border formation of osteoclasts. *J. Biol. Chem* **280**, 32356-32361.

van Ijzendoorn, S. C., Mostov, K. E. and Hoekstra, D. (2003). Role of rab proteins in epithelial membrane traffic. *Int. Rev. Cytol.* **232**, 59-88.

Verhoeven, K., De Jonghe, P., Coen, K., Verpoorten, N., Auer-Grumbach, M., Kwon, J. M., FitzPatrick, D., Schmedding, E., De Vriendt, E., Jacobs, A. et al. (2003). Mutations in the small GTP-ase late endosomal protein RAB7 cause Charcot-Marie-Tooth type 2B neuropathy. *Am. J. Hum. Genet.* **72**, 722-727.

Vitelli, R., Santillo, M., Lattero, D., Chiariello, M., Bifulco, M., Bruni, C. and Bucci, C. (1997). Role of the small GTPase Rab7 in the late endocytic pathway. *J. Biol. Chem.* **272**, 4391-4397.

Wang, T. and Hong, W. (2002). Interorganellar regulation of lysosome positioning by the Golgi apparatus through Rab34 interaction with Rab-interacting lysosomal protein. *Mol. Biol. Cell* **13**, 4317-4332.

Wang, Y., Chen, T., Han, C., He, D., Liu, H., An, H., Cai, Z. and Cao, X. (2007). Lysosome-associated small Rab GTPase Rab7b negatively regulates TLR4 signaling in macrophages by promoting lysosomal degradation of TLR4. *Blood* **110**, 962-971.

Ward, T. H., Polishchuk, R. S., Caplan, S., Hirschberg, K. and Lippincott-Schwartz, J. (2001). Maintenance of Golgi structure and function depends on the integrity of ER export. *J. Cell Biol.* **155**, 557-570.

Yamashiro, D. J. and Maxfield, F. R. (1984). Acidification of endocytic compartments and the intracellular pathways of ligands and receptors. *J. Cell Biochem.* **26**, 231-246.

Yang, M., Chen, T., Han, C., Li, N., Wan, T. and Cao, X. (2004). Rab7b, a novel lysosome-associated small GTPase, is involved in monocytic differentiation of human acute promyelocytic leukemia cells. *Biochem. Biophys. Res. Commun.* **318**, 792-799.

Yao, M., Liu, X., Li, D., Chen, T., Cai, Z. and Cao, X. (2009). Late endosome/lysosome-localized Rab7b suppresses TLR9-initiated proinflammatory cytokine and type I IFN production in macrophages. *J. Immunol.* **183**, 1751-1758.

Journal of Cell Science